Asian Journal of Immunology

Volume 8, Issue 1, Page 269-284, 2025; Article no.AJI.147582

An Immunocomputing Approach to the Development of Multiepitope Vaccine against *Mycobacterium tuberculosis*

Naseema. R [a*]

[a] *Department of Biotechnology, Mepco Schlenk Engineering College, Sivakasi, Tamil Nadu, India.*

Author's contribution

The sole author designed, analyzed, interpreted and prepared the manuscript.

Article Information

DOI: https://doi.org/10.9734/aji/2025/v8i1178

Open Peer Review History:
This journal follows the Advanced Open Peer Review policy. Identity of the Reviewers, Editor(s) and additional Reviewers, peer review comments, different versions of the manuscript, comments of the editors, etc are available here: https://pr.sdiarticle5.com/review-history/147582

Original Research Article

Received: 17/09/2025
Published: 24/11/2025

ABSTRACT

Tuberculosis (TB) is the second most deadly airborne infectious disease caused by *Mycobacterium tuberculosis*, posing a major global health risk dw. Nearly one-third of the world's population is infected, with low-income countries most affected due to limited access to diagnostics and treatments. Although the Bacillus Calmette–Guérin (BCG) vaccine offers protection in infancy, its reduced efficacy beyond 20 years limits long-term TB control. This study focuses on drafting a multi-epitope peptide-based vaccine against TB using immune-informatics approaches. Ten *M. tuberculosis*-specific antigenic proteins (PPE39, PPE68, Rv0310c, PE_PGRS35, PE_PGRS31, CFP10, Rv1975, lpqG, esxV, and espJ) were analyzed to identify potent immunogenic regions. Five cytotoxic T lymphocyte (CTL) epitopes, five helper T cell (HTL) epitopes, and several B-cell epitopes are proficient of causing strong immune responses, including Interferon-γ (IFN-γ) production, were selected. A total of 27 epitopes were linked using AAY, GPGPG, and KK linkers to construct the vaccine, which was assessed for physicochemical properties, antigenicity, allergenicity, and toxicity. The design demonstrated stability and strong immunogenic potential. Molecular docking with the TLR-4 monomer showed favorable binding affinity, indicating its

**Corresponding author: E-mail: naseemar8@gmail.com;*

Cite as: *Naseema. R. 2025. "An Immunocomputing Approach to the Development of Multiepitope Vaccine Against Mycobacterium Tuberculosis". Asian Journal of Immunology 8 (1):269–284. https://doi.org/10.9734/aji/2025/v8i1178.*

potential as an effective vaccine candidate. By applying immune-informatics tools for precise epitope selection and vaccine design, this research provides a cost-effective strategy to enhance TB prevention. The study offers a strong framework for developing next-generation TB vaccines and supports global efforts to eliminate tuberculosis by 2035.

Keywords: Mycobacterium tuberculosis (M.tb); Cytotoxic T lymphocyte (CTL); Helper T cell (HTL); Interferon-γ (IFN-γ); Bacillus Calmette–Guérin (BCG).

1. INTRODUCTION

"Tuberculosis (TB) is an airborne disease caused by the bacterium *Mycobacterium tuberculosis*. *M. tb* and its seven closely related species namely *M. bovis*, *M. africanum*, *M. microti*, *M. caprae*, *M. pinnipeti*, *M. canetti* and *M. munji* collectively comprises *M. tuberculosis* complex. But not all of these species are reported to cause disease in humans" (Beresford & Sadoff, 2010). "The majority cases of TB are found to be caused by *M. tuberculosis* (Wheeler et al., 2007). TB remains one among the main global health threats which causes millions of deaths annually across the globe. Majority of affected people hail from low income and middle-income countries (LMIC) like countries from African sub- continent" (Faust et al., 2019). "An estimated 10 million people fell ill with TB worldwide in 2019, which includes 5.6 million men, 3.2 million women, and 1.2 million children" (Saha & Raghava, 2006). "TB is existing in all Countries and all age groups. 5 – 15 % patients infected with only TB are likely to develop active TB in their lifetime. TB is more severe in HIV patients and is one of the main reason for their mortality. BCG (Bacille Calmette - Guerin) is the only vaccine available for preventing TB in humans. Although BCG is of low-cost and widely used vaccine in many of the countries, its potency has varied generally in many clinical assays spanned between 0- 80 % (Brandt et al., 2002; Pablos-Mendez et al., 2002). It offers poor protection in adults and adolescents against pulmonary tuberculosis" (Ferraz et al., 2004). Also failed to treat Latent TB infection (LTBI) (Weinreich Olsen et al., 2000). In the presence of immune-suppression, reversion of virulence may take place and possible induction of disease may happen (Sharma et al., 2021). For these various reasons, the WHO has framed "The End TB Strategy which targets the prevention, care and control for Tuberculosis. To meet all the requirements and to satisfy all the problems associated with *Mycobacterium tuberculosis*, there is an urge to build an efficient vaccine, which offers complete safeguard against tuberculosis" (World Health Organization, 2018).

"In the current study, we have chosen ten mycobacterial proteins from different region of difference (PPE39, PPE68, Rv0310c, PE_PGRS35, PE_PGRS_31, CFP10, Rv1975, lpqG, esxV, espJ) and an adjuvant (RpfE) for vaccine construct. PE/PPE families are found to be associated with pathogenicity of MTB infection. As in all pathogenic mycobacteria, the members of these families are abundant and comparatively shows less presence in non-pathogenic mycobacteria. It is observed that, PE/PPE proteins play a major role in processing of macrophages" (Bigi et al., 2000). Adhesion of pathogenic proteins on the surface of macrophage receptors, immune response to pathogenic proteins, resistance of intracellular stress, Phagocytosis, intracellular survival in the host environment and regulation of cell fate are the key events involved in the Host-Pathogen interactions.

During various stages of infection, the CFP10/ESAT6 complex in *Mycobacterium tuberculosis* could play a role in regulating macrophage death (Trott & Olson, 2010). "The major advantage in peptide-based vaccines is the absence of live or attenuated infectious materials. Hence there is zero risk for reversion of virulence" (Trunz et al., 2006). "To enhance the stability, solubility lipid, carbohydrate and phosphates groups can be readily introduced. One major advantage of epitope-based vaccines is that they rely on a small, precisely defined antigen, making it easier to understand and evaluate its immunogenicity and antigenicity (Choi et al., 2015). The induction of neutralizing antibodies and a protective T helper and a CTL response by T cell and B cell epitope must be required for a good TB vaccine. To maximize coverage, the CTL and HTL epitopes were tested for their ability to bind with the most prevalent human HLA alleles for MHC class I and II (Martinot et al., 2016). "The adjuvant RfpE was included to the vaccine draft to enhance its immunogenicity" (Bellini & Horváti, 2020). Several vaccine sequences were generated and analyzed for allergenicity, toxicity, antigenicity, and important physicochemical properties such

as isoelectric point, solubility, and half-life in different hosts" (Kelley et al., 2015). "Homology modeling was carried out for all vaccine sequences, and the best 3D model was chosen based on the recommendations of online servers" (Rapin et al., 2010). The stereochemical geometry of this model was then evaluated, both at the residue level and overall structure (Sanches et al., 2021). Finally, molecular docking was performed between the optimized 3D vaccine model and TLR4 to study binding interactions.

2. METHODS AND METHODOLOGY

1. HTL epitopes prediction:

Helper T lymphocyte (HTL) epitopes were forecasted using the NetMHCIIpan 4.0 server, which is an online tool for identifying immune epitopes based on a large collection of experimentally validated data. All protein sequences of the chosen antigens were handed in simultaneously in FASTA format. The default settings were used to predict epitopes across the total human HLA reference set, specifying an epitope length of 9 amino acids. The predicted epitopes were then ranked and scored according to their binding affinity.

2. CTL epitopes prediction:

Cytotoxic T lymphocyte (CTL) epitopes were predicted using the NetCTLpan 1.2 server. All amino acid sequences from the selected proteins were uploaded together in FASTA format. Using the full human HLA reference set, 9-mer epitopes were predicted with default settings, and the resulting peptides were ranked by their scores. The chosen epitopes were then examined for their allergenic, toxic, and antigenic properties.

MHC I–related HLA-C epitopes were identified with the NetCTLpan 1.1 server, with all selected protein sequences submitted at once in FASTA format.This prediction is based on MHC class – I binding affinity, proteasomal cleavage efficiency and TAP transport efficiency. 20 alleles of HLA-C haplotype were given as input for prediction. These 20 alleles were taken as a reference set from IEDB. In total five HLA -C epitopes were chosen for the vaccine construct.

3. B-cell epitopes prediction:

The B cell epitopes were predicted using ABCpred web server. All the amino acids sequences of the selected proteins were submitted at a time in fasta format (Hougardy et al., 2007). The top 30 epitopes were selected based on the score and was further analyzed for antigenicity, toxicity and allergenicity. Any epitopes flagged as allergenic, toxic, or non-antigenic by AllerTop v2.0, ToxinPred, or VaxiJen were not included in the study. Altogether, fourteen B-cell epitopes were chosen from the ten selected proteins (Supplementary Table 1).

4. IFN-γ analysis:

IFN-γ plays a central role in defending the body against intracellular pathogens, and in *Mycobacterium tuberculosis* infection it is especially important for activating macrophages (Dimitrov et al., 2014). The IFN were predicted from the IFN epitope server (http://crdd.osdd.net/raghava/ifnepitope/). Here, we analyzed IFN-γ activity for all the selected epitopes.

5. Vaccine construct preparation:

Five vaccine constructs were randomly designed using the adjuvant (RpfE), which was attached to the N-terminal end. Each construct followed the same layout, placing B-cell, HTL, CTL, and then HLA-C epitopes in sequence. The epitopes were joined using KK, GPGPG, and AAY linkers, and the adjuvant was added using an EAAAK linker.

6. Prediction of epitope's antigenicity, allergenicity and toxicity:

Five vaccine constructs were randomly designed using the adjuvant RpfE, which was attached to the N-terminal end. In each construct, the selected epitopes were arranged in the order of B-cell, HTL, CTL, and HLA-C. The B-cell, HTL, CTL, and HLA-C epitopes were joined using KK, GPGPG, and AAY linkers, respectively, while the adjuvant was connected through an EAAAK linker, the relative abundance of amino acids, and β-strand forming propensity (Doytchinova & Flower, 2007). Prediction of antigenicity was done by alignment-independent fashion based on its physicochemical properties using VaxiJen online web server (Gupta et al., 2013). This tool provided varied options for the organism selected for analysis was *bacteria*, for which the corresponding default threshold score (0.4) was applied automatically. The ToxinPred server was employed to assess the toxicity of the selected sequences, as this tool generates all possible

mutants of the input peptides for evaluation (Branger et al., 2004). All parameters in both AllerTOP v.2.0 and ToxinPred were maintained at their default settings.

7. Homology modelling of vaccine constructs:

The five vaccine constructs were analyzed through homology modelling on the SWISS-MODEL server to identify the most structurally stable option. The generated models were saved in PDB format for later evaluation.

8. Structure Refinement of Vaccine Construct:

The tertiary structure of the selected vaccine draft was refined utilizing the CASTp web server. CASTp applies structural perturbation and molecular dynamics simulations to achieve protein relaxation. The most stable and accurately refined model was selected for further evaluation, including physicochemical property assessment and molecular docking studies.

9. Physiochemical properties of vaccine construct:

The physicochemical characteristics of the vaccine construct were found using the ProtParam tool available online. This tool evaluates several properties of a protein, including molecular weight, theoretical isoelectric point (pI), instability index, protein length, estimated half- life, aliphatic index, and the grand average of hydropathicity (GRAVY).

10. Molecular docking of vaccine construct:

The refined 3D structures of the vaccine constructs were utilized for molecular docking studies. The crystal structure of the human TLR4 receptor complex (PDB ID: 3FXI) was retrieved from the Protein Data Bank. Docking was performed using the PyDock web server with the monomeric form of the human TLR4 receptor (Schorey & Harding, 2016). Additionally, AutoDock Vina was employed to perform docking using the A-chain of the TLR4 crystal structure with the vaccine constructs (Park et al., 2009; Heo et al., 2013). Using the CASTp server, we identified the active and passive binding pockets of the TLR4 receptor and the refined vaccine constructs. The corresponding PDB files were then uploaded to the PyDock server for docking analysis.

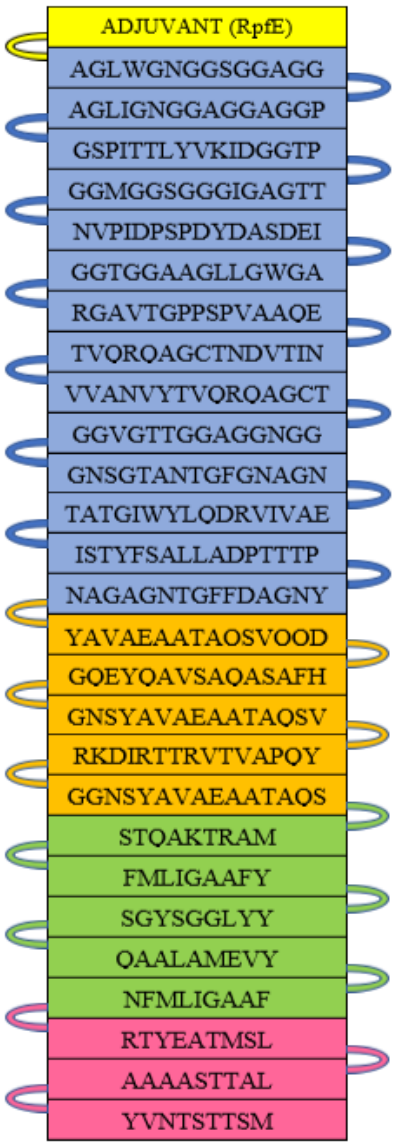

Fig. 1. The schematic illustration of the final vaccine construct shows the arrangement of epitopes, represented within colored boxes and connected by linker sequences. The designed construct is made up of 623 amino acids, including a 172-amino-acid adjuvant (RpfE/Rv2450c) highlighted in yellow. It incorporates 14 B-cell epitopes (blue), 5 HTL epitopes (orange), 5 CTL epitopes (green), and 3 HLA-C epitopes (pink). An EAAAK linker attaches the adjuvant to the N-terminus, while the B-cell, HTL, CTL, and HLA-C epitopes are connected using KK, GPGPG, and AAY linkers

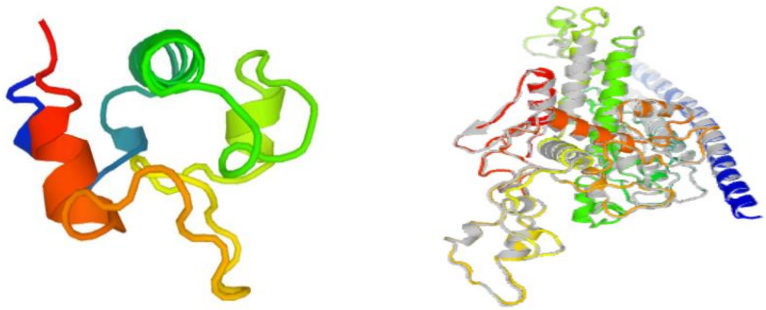

A) B)

Fig. 2. Vaccine construct homology modelling and structural refinement: (A) The RpfE vaccine construct's three-dimensional structure was first created using SWISS-MODEL (B) Refined version was produced using CASTp (Binkowski et al., 2003)

11. Immune simulation for vaccine efficacy

"C-ImmSim was used to assess the immune response and immunogenicity of the multi-epitope vaccine. The server applies a position-specific scoring matrix and machine learning, along with epitope prediction, to model immune interactions. It contains 6,533 antigenic epitopes and 33 different human HLA allele sets, simulating responses by pairing epitope sequences with lymphocyte receptors" (Brosch et al., 2007). "The tool predicts immune responses by simulating three important mammalian anatomical regions: the thymus, bone marrow, and a tertiary lymphoid organ, including the spleen, lymph nodes, or tonsils (Mangtani et al., 2014). The vaccine construct and the PDB files for TLR4 and MHC I were uploaded to C-ImmSim, using the default settings for all parameters.

3. RESULTS

1. B-cell epitopes prediction:

A total of thirty B-cell epitopes were first predicted with ABCPred and then evaluated for their antigenic, toxic, and allergenic properties. Epitopes identified as toxic, allergenic, or non-antigenic through ToxinPred, AllerTOP v.2.0, and VaxiJen, respectively, were excluded from further analysis. Ultimately, fourteen B-cell epitopes were selected for inclusion in the vaccine construct.

2. HTL epitopes prediction:

From the initial set of twenty predicted HTL epitopes, only those exhibiting antigenic, non-toxic, and non-allergenic properties were considered. Using these criteria, five HTL epitopes were selected for inclusion in the vaccine construct.

3. CTL epitopes prediction:

Twenty CTL epitopes with the highest binding affinity to MHC class I molecules were selected for further evaluation of allergenicity, antigenicity, and toxicity. Any duplicate epitopes found across multiple HLA sets were removed. Only epitopes that were non-allergenic, non-toxic, and antigenic were retained for downstream analyses. In total, five CTL epitopes and three HLA-C epitopes derived from *PPE39*, *PPE68*, *Rv0310c*, *PE_PGRS35*, *PE_PGRS31*, *CFP10*, *Rv1975*, *lpqG*, *esxV*, and *espJ* were selected for vaccine construction.

4. Vaccine construct preparation:

Two random vaccine constructs were generated by shuffling the arrangement of the selected epitopes. In each construct, the epitopes were organized in the order of B-cell, HTL, CTL, and HLA-C. The B-cell, HTL, CTL, and HLA-C epitopes were connected using KK, GPGPG, and AAY linkers, respectively. The adjuvant proteins RpfE and RpfB were attached to the N-terminal end of the vaccine constructs via an EAAAK linker.

5. Homology modelling and selection of best vaccine construct:

Homology modelling and structural validation of the vaccine constructs were performed using the SWISS-MODEL web server. The generated models were evaluated based on the Ramachandran plot statistics, mean score, and

Z-score provided by SWISS-MODEL reports. Among all constructs, Vaccine Construct 1 exhibited the most favorable results, with residues in the most preferred regions, additionally allowed regions, generously allowed regions, and disallowed regions accounting for 93.06%, 5.17%, 1.77%, and 0.0%, respectively. While the Z-score, RMSD, MolProbity, clash score for Verify3D were -1.10,0.248,1.39 and 6.9 respectively. The final chosen vaccine construct was also analyzed for its antigenicity using VaxiJen tool where antigenicity was predicted to be 1.0664. The chosen vaccine construct sequence is shown in Supplementary Fig.1 and the graphical representation of vaccine construct in order of epitopes utilized can be found in Fig. 1.

6. Vaccine construct tertiary structure refinement:

The homology model generated using Swiss model (Fig. 2A) is exhibiting the finest Ramachandran plot values was exposed to improvement using CastP. Out of all the five models generated by CastP, model 2 (Fig. 2B) was found to be most appropriate where values for GDT-HA, RMSD and MOLProbity were 0.993, 0.248 and 1.378 respectively. After refinement, the most preferred regions of Ramachandran increased to 93.72% when compared to the structure obtained from Swiss model (Fig.3). At last, the refined model 2 was chosen for further investigations like molecular docking and dynamic simulations.

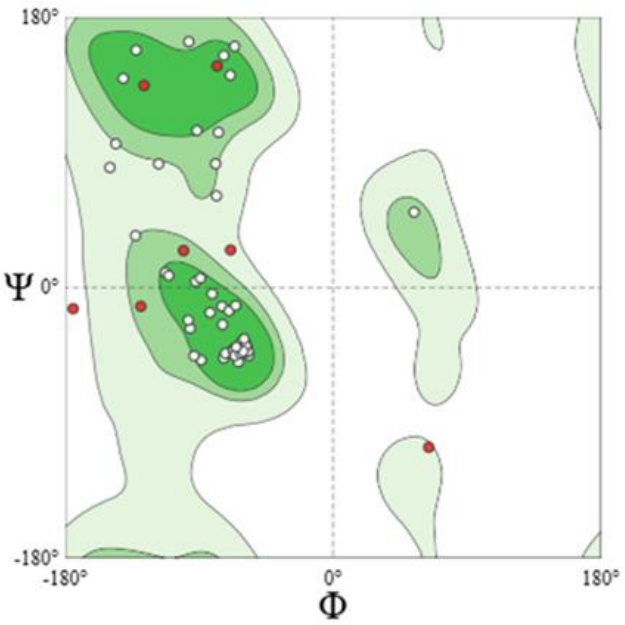

Name	Value
MolProbity Score	1.39
Clash Score	0.00
Ramachandran Favoured	93.06%
Ramachandran Outliers	2.78% (A143 ASN – 0.0271; A133 ARG – 0.0079)
Rotamer Outliers	3.85% (A115 ILE – 0.0346; A109 SER – 0.0156)
C-Beta Deviations	1 (A142 ALA – 0.2939)
Bad Bonds	0 / 566
Bad Angles	3 / 767 (A141 ALA–A142 ALA – 5.70σ; A142 ALA–A143 ASN – 4.50σ; A135 ASN – 4.30σ)
Cis Non-Proline	1 / 72 (A141 ALA–A142 ALA – Omega −6.22°)
MolProbity Version	4.4

Fig. 3. Ramachandran plot analysis of the refined tertiary structure of vaccine construct obtained from rampage web server. After refinement, most preferred regions increased to 93.72% as compared to the crude 3D structure derived from Swiss model where the most favoured regions were 93.06%

7. Vaccine constructs physicochemical properties:

The selected refined vaccine construct consisted of 623 amino acids with an estimated molecular weight of 61.83 kDa. Typically, vaccine candidates with molecular masses greater than 50 kDa are preferred, as those with lower molecular weights tend to exhibit reduced lymph node accumulation. The construct has a theoretical pI of 9.10, containing 39 negatively and 49 positively charged residues, suggesting a basic nature. Its predicted half-life is around 30 hours in mammalian reticulocytes, over 10 hours in *E. coli*, and over 20 hours in yeast. The aliphatic index was determined to be 60.42, and the instability index was 31.42, suggesting that the protein is thermally stable. The grand average of hydropathicity (GRAVY) value was calculated as −0.282, indicating the hydrophilic nature of the construct.

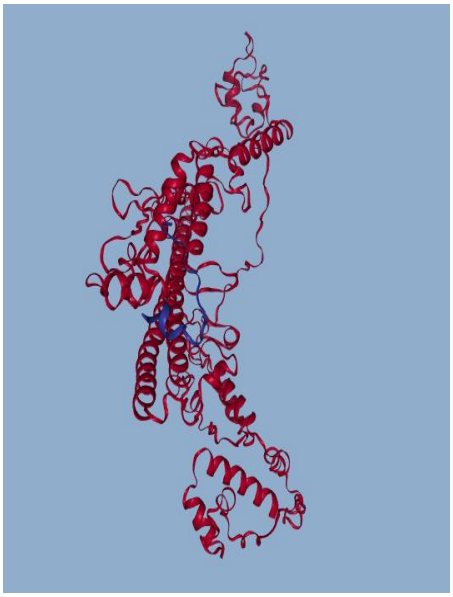

Fig. 4. Molecular docking of vaccine construct and TLR4 ligand

8. Molecular docking of vaccine construct with TLR4:

The CASTp server was employed to identify the active and passive ligand-binding sites within the refined tertiary structure of the vaccine construct (Gülbay et al., 2006). The analysis revealed 62 active and 91 passive ligand-binding residues in TLR4. For the vaccine construct, 129 residues were identified as active and 145 as passive binding sites. Both the refined construct and TLR4 monomers were subsequently submitted to the PyDock server for molecular docking. PyDock provided top 10 models in which model 1 was selected. Other calculated parameters are provided in Supplementary Table 2. The docked vaccine construct and TLR4 receptor can be seen in Fig. 4.

9. Molecular docking of vaccine construct with MHC I:

To predict the active and passive ligand binding sites in the refined tertiary vaccine structure the CastP server was used (Martinot et al., 2016). It predicted 60 residues as active ligand- binding sites and 92 residues as passive ligand- binding sites for MHC I. The predicted active ligand-binding sites and passive ligand-binding sites for vaccine construct was 129, 145 residues respectively. For molecular docking, the refined vaccine construct and MHC I monomers were uploaded to PyDock web server. PyDock provided top 10 models in which model 1 was selected. Other calculated parameters are provided in Supplementary Table 3. The docked vaccine draft and MHC I receptor can be seen in Fig. 5.

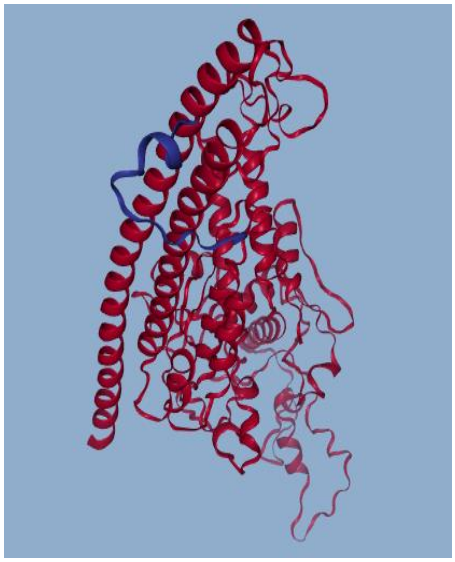

Fig. 5. Molecular docking of vaccine construct and MHC I ligand

10. Immune simulation for vaccine efficacy

The immune responses predicted by the C-ImmSim server indicated a robust immunogenic potential for the vaccine construct. The vaccine elicited strong primary and secondary immune responses, as reflected in the simulation graphs. The primary response was characterized by an

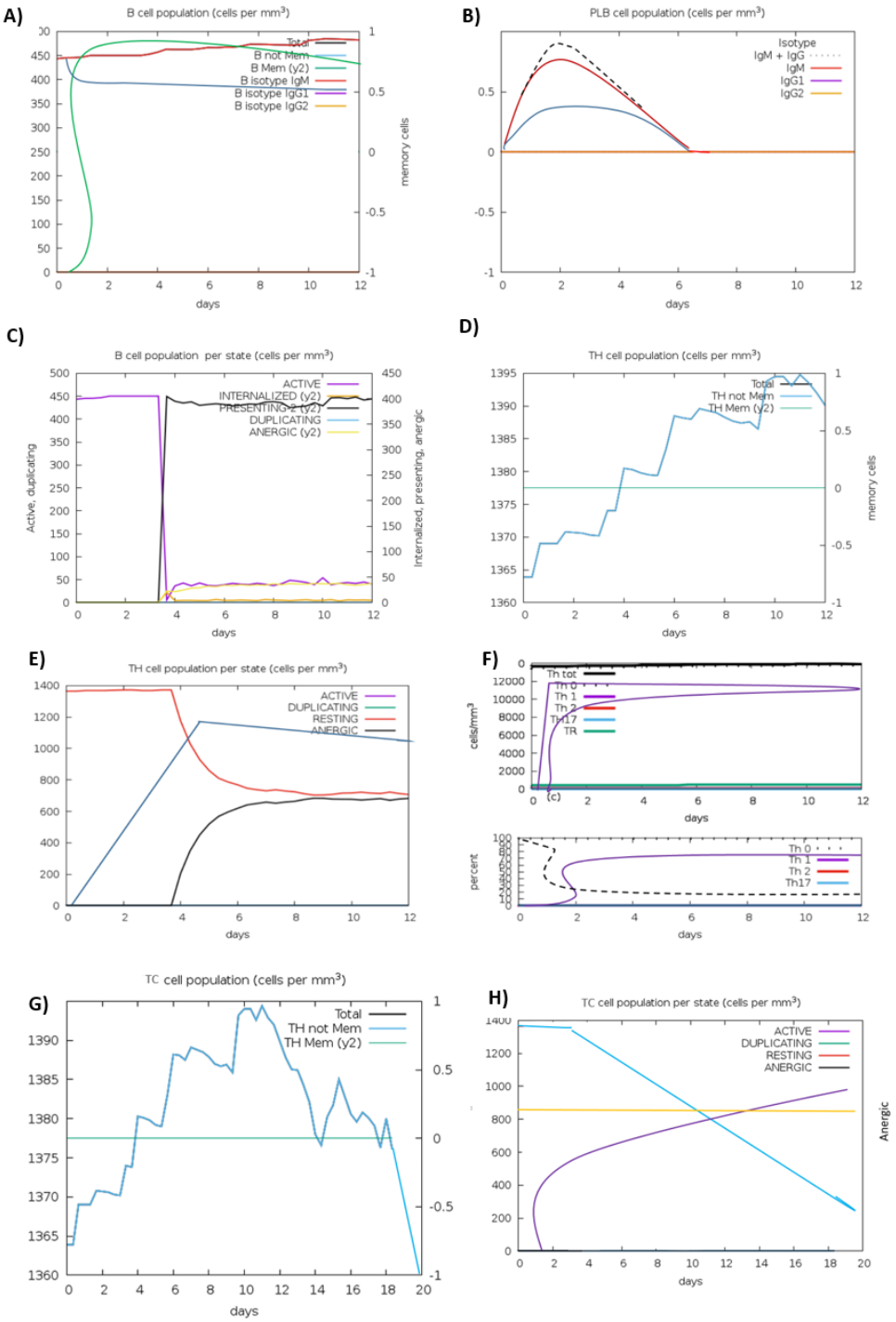

Fig. 6. *In silico* immune simulation results of vaccine construct with TLR4 ligand using C-ImmSim web server (https:// www. iac. cnr. it/ ~filip po/ proje cts/c- immsim- online. html). (A) The rapid expansion of B-cells was accompanied by the formation of memory B-cells. (B) Elevated level IgG +IgM antibodies in peripheral blood cells. (C) Elevated B-cell (active) production after a lag phase of 5–7 days after exposure to the vaccine chimera. (D) High level of T helper cells production in response to antigens (E)Active T helper cell population within 5 days of exposure to antigen. (F) Constant production of Th1 cells (G) Increased level of cytotoxic T memory cells and (H) Evolution of cytotoxic T-cells

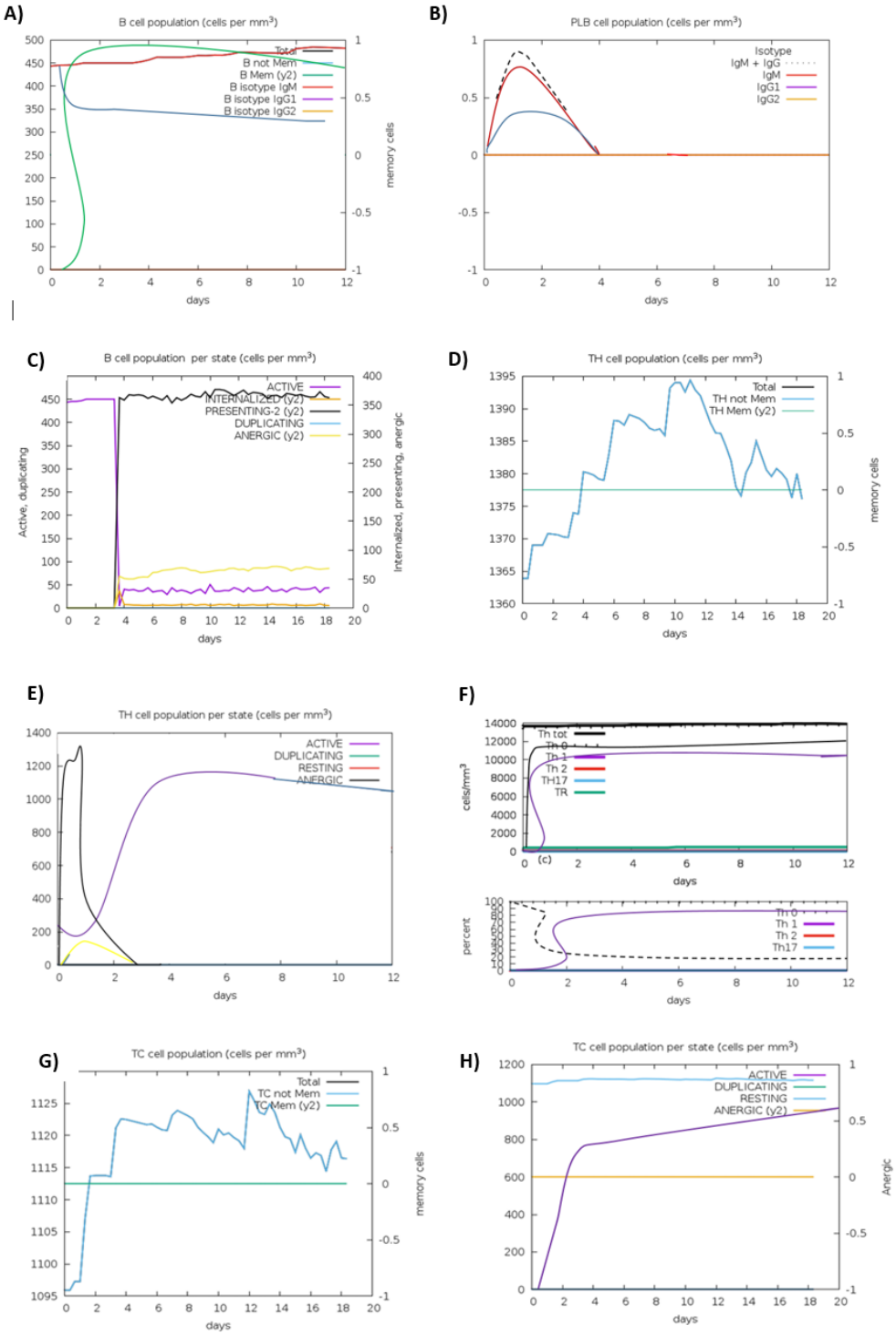

Fig. 7. *In silico* immune simulation results of vaccine construct with MHC I ligand using C-ImmSim web server (https:// www. iac. cnr. it/ ~filip po/ proje cts/c- immsim- online. html). (A) The rapid proliferation of B-cell along with memory B-cells. (B) High level of IgG +IgM antibodies in peripheral blood cells. (C) Increased B-cell (active) production after a lag phase of 5–7 days after exposure to the vaccine chimera. (D) Elevated level of T helper cells production in response to antigens (E)Active T helper cell population within 5 days of exposure to antigen. (F) Constant production of Th1 cells (G) Higher level of cytotoxic T memory cells and (H) Evolution of cytotoxic T-cells

increase in IgM antibody levels following a lag period of 5–7 days post-antigen exposure. The secondary response demonstrated enhanced B-cell proliferation along with elevated levels of IgG+IgM, IgM, and IgG1+IgG2 antibodies. In addition to promoting significant B-cell proliferation and memory B-cell formation, the vaccine construct induced strong cytotoxic and helper T-cell activity and maintained elevated IFN-γ levels for an extended duration.

4. DISCUSSION

Mycobacterium tuberculosis (*M. tb*) is the second deadliest disease which can actively tackle antibiotic treatment (Mehla & Ramana, 2016). “Globally, there is an urge to develop vaccines and treatment for TB, because recently it has been identified that the well-known and only licensed anti-tuberculosis vaccine called BCG is no longer effective in adults” (Mustafa, 2002). “In light of ever-growing drug resistance and adverse effects associated with anti-TB drugs such as ototoxicity, hepatotoxicity, neuro-psychiatricevents, hyperuricemia, gastrointestinal disturbance, vision loss, skin pigmentation etc, a safe and efficacious vaccine could be an imperious arsenal against this lethal disease” (Nagpal et al., 2020). “The different protocols followed by various laboratories over the last few years for BCG culture showed different level of divergence in the efficacy of BCG vaccine” (Lee et al., 2014). “Several reports suggest that BCG grown in Sauton medium elicits a stronger immune response than BCG cultured in Middlebrook 7H9 medium” (Fleri et al., 2017). “Out of the numerous anti-tuberculosis vaccines under development, only VMP1002, MIP, and *M. vaccae* have advanced to phase III trials, with plans to use them as boosters for BCG in the future. In recent years, the use of immunoinformatics has rapidly gained attention for drug and vaccine development compared to traditional approaches” (Jung et al., 2011). In this study, a multi-epitope vaccine was designed using experimentally validated immunogenic exosome vesicle-based antigens in response to the global crisis (Carmona et al., 2013). “To assess their immune-stimulating potential, these antigens were examined for B-cell, HTL, and CTL epitopes, corresponding to humoral, innate, and cell-mediated responses. Additionally, all selected epitopes were evaluated for non-toxicity, non-allergenicity, and IFN-γ induction. The chosen epitopes were linked using appropriate peptide linkers, and the TLR4 agonist peptide RpfE was attached to the N-terminal of the construct to serve as an adjuvant and enhance the immune response. During *M. tuberculosis* infection, both TLR2 and TLR4 are involved in pathogen recognition, activating macrophages and dendritic cells and influencing both innate and adaptive immunity” (Hart et al., 1987). “TLR4 was selected as the target receptor for the vaccine construct due to its critical role in infection; TLR4-deficient mice show lower survival rates and higher bacterial loads compared to TLR2-deficient mice when infected with *M. tuberculosis”* (Kim et al., 2018). Five vaccine constructs were created and evaluated using homology modeling. One construct was refined in 3D and docked with monomeric TLR4, producing a complex with favorable binding energy and stable structure. Finally, an immune simulation study, modeling the innate immune network including T and B cells, was performed to evaluate both humoral and cellular responses. The results indicate that the designed multi-epitope vaccine elicits a strong and consistent immune response.

5. CONCLUSION

Our results show that the vaccine candidate possesses suitable physicochemical qualities, a stable structure, and encouraging immunological attributes capable of promoting both humoral and cellular immunity. Building upon these findings, future work will focus on validating the efficacy of the proposed vaccine as both a preventive and therapeutic candidate through in vivo evaluation in a suitable mouse model. Therefore, it should be pushed forward as a potential lead candidate for in vivo and in vitro assessments against *M. tb*. (Yun et al., 2024; Nayak et al., 2023).

DISCLAIMER (ARTIFICIAL INTELLIGENCE)

Author(s) hereby declare that NO generative AI technologies such as Large Language Models (ChatGPT, COPILOT, etc) and text-to-image generators have been used during writing or editing of this manuscript.

COMPETING INTERESTS

Authors have declared that no competing interests exist.

REFERENCES

Bellini, C., & Horváti, K. (2020). Recent advances in the development of protein- and peptide-

based subunit vaccines against tuberculosis. *Cells, 9*(12), 2673.

Beresford, B., & Sadoff, J. C. (2010). Update on research and development pipeline: tuberculosis vaccines. *Clinical Infectious Diseases, 50*(Suppl. 3), S178–S183.

Bigi, F., Alito, A., Romano, M. I., Zumarraga, M., Caimi, K., & Cataldi, A. (2000). The gene encoding P27 lipoprotein and a putative antibiotic-resistance gene form an operon in *Mycobacterium tuberculosis* and *Mycobacterium bovis*. *Microbiology, 146*(4), 1011–1018.

Binkowski, T. A., Naghibzadeh, S., & Liang, J. (2003). CASTp: Computed atlas of surface topography of proteins. *Nucleic Acids Research, 31*(13), 3352–3355.

Brandt, L., Cunha, J. F., Olsen, A. W., Chilima, B., Hirsch, P., Appelberg, R., & Andersen, P. (2002). Failure of the *Mycobacterium bovis* BCG vaccine: Some species of environmental mycobacteria block multiplication of BCG and induction of protective immunity to tuberculosis. *Infection and Immunity, 70*(2), 672–678.

Branger, J., Leemans, J. C., Florquin, S., Weijer, S., Speelman, P., & Van Der Poll, T. (2004). Toll-like receptor 4 plays a protective role in pulmonary tuberculosis in mice. *International Immunology, 16*(3), 509–516.

Brosch, R., et al. (2007). Genome plasticity of BCG and impact on vaccine efficacy. *Proceedings of the National Academy of Sciences, 104*, 5596–5601.

Carmona, J., Cruz, A., Moreira-Teixeira, L., Sousa, C., Sousa, J., Osorio, N. S., Saraiva, A. L., et al. (2013). *Mycobacterium tuberculosis* strains are differentially recognized by TLRs with an impact on the immune response. *PLoS One, 8*(6), e67277.

Choi, H.-G., Kim, W. S., Back, Y. W., Kim, H., Kwon, K. W., Kim, J.-S., Shin, S. J., & Kim, H.-J. (2015). *Mycobacterium tuberculosis* RpfE promotes simultaneous Th1- and Th17-type T-cell immunity via TLR4-dependent maturation of dendritic cells. *European Journal of Immunology, 45*(7), 1957–1971.

Dimitrov, I., Bangov, I., Flower, D. R., & Doytchinova, I. (2014). AllerTOP v. 2—a server for in silico prediction of allergens. *Journal of Molecular Modeling, 20*(6), 1–6.

Doytchinova, I. A., & Flower, D. R. (2007). VaxiJen: A server for prediction of protective antigens, tumour antigens and subunit vaccines. *BMC Bioinformatics, 8*(1), 1–7.

Faust, L., Schreiber, Y., & Bocking, N. (2019). A systematic review of BCG vaccination policies among high-risk groups in low TB-burden countries: Implications for vaccination strategy in Canadian indigenous communities. *BMC Public Health, 19*(1), 1–32.

Ferraz, J. C., Stavropoulos, E., Yang, M., Coade, S., Espitia, C., Lowrie, D. B., Colston, M. J., & Tascon, R. E. (2004). A heterologous DNA priming-*Mycobacterium bovis* BCG boosting immunization strategy using mycobacterial Hsp70, Hsp65, and Apa antigens improves protection against tuberculosis in mice. *Infection and Immunity, 72*(12), 6945–6950.

Fleri, W., Paul, S., Dhanda, S. K., Mahajan, S., Xu, X., Peters, B., & Sette, A. (2017). The immune epitope database and analysis resource in epitope discovery and synthetic vaccine design. *Frontiers in Immunology, 8*, 278.

Gülbay, B. E., Gürkan, Ö. U., Yıldız, Ö. A., Önen, Z. P., Erkekol, F. Ö., Baççıoğlu, A., & Acıcan, T. (2006). Side effects due to primary antituberculosis drugs during the initial phase of therapy in 1149 hospitalized patients for tuberculosis. *Respiratory Medicine, 100*(10), 1834–1842.

Gupta, S., Kapoor, P., Chaudhary, K., Gautam, A., Kumar, R., Open Source Drug Discovery Consortium, & Raghava, G. P. S. (2013). In silico approach for predicting toxicity of peptides and proteins. *PLoS One, 8*(9), e73957.

Hart, P. D., Young, M. R., Gordon, A. H., & Sullivan, K. H. (1987). Inhibition of phagosome-lysosome fusion in macrophages by certain mycobacteria can be explained by inhibition of lysosomal movements observed after phagocytosis. *The Journal of Experimental Medicine, 166*(4), 933–946.

Heo, L., Park, H., & Seok, C. (2013). GalaxyRefine: Protein structure refinement driven by side-chain repacking. *Nucleic Acids Research, 41*(W1), W384–W388.

Hougardy, J.-M., Schepers, K., Place, S., Drowart, A., Lechevin, V., Verscheure, V., Debrie, A.-S., et al. (2007). Heparin-binding-hemagglutinin-induced IFN-γ release as a diagnostic tool for latent tuberculosis. *PLoS ONE, 2*(10), e926.

Jung, I. D., Jeong, S. K., Lee, C.-M., Noh, K. T., Heo, D. R., Shin, Y. K., Yun, C.-H., et al.

(2011). Enhanced efficacy of therapeutic cancer vaccines produced by co-treatment with *Mycobacterium tuberculosis* heparin-binding hemagglutinin, a novel TLR4 agonist. *Cancer Research, 71*(8), 2858–2870.

Kelley, L. A., Mezulis, S., Yates, C. M., Wass, M. N., & Sternberg, M. J. E. (2015). The Phyre2 web portal for protein modeling, prediction and analysis. *Nature Protocols, 10*(6), 845–858.

Kim, W. S., Jung, I. D., Kim, J.-S., Kim, H. M., Kwon, K. W., Park, Y.-M., & Shin, S. J. (2018). *Mycobacterium tuberculosis* GrpE, a heat-shock stress responsive chaperone, promotes Th1-biased T cell immune response via TLR4-mediated activation of dendritic cells. *Frontiers in Cellular and Infection Microbiology, 8*, 95.

Lee, S. J., Shin, S. J., Lee, M. H., Lee, M.-G., Kang, T. H., Park, W. S., Soh, B. Y., et al. (2014). A potential protein adjuvant derived from *Mycobacterium tuberculosis* Rv0652 enhances dendritic cells-based tumor immunotherapy. *PLoS One, 9*(8), e104351.

Mangtani, P., Abubakar, I., Ariti, C., Beynon, R., Pimpin, L., Fine, P. E. M., Rodrigues, L. C., et al. (2014). Protection by BCG vaccine against tuberculosis: A systematic review of randomized controlled trials. *Clinical Infectious Diseases, 58*(4), 470–480.

Martinot, A. J., Farrow, M., Bai, L., Layre, E., Cheng, T.-Y., Tsai, J. H., Iqbal, J., et al. (2016). Mycobacterial metabolic syndrome: LprG and Rv1410 regulate triacylglyceride levels, growth rate and virulence in *Mycobacterium tuberculosis*. *PLoS Pathogens, 12*(1), e1005351.

Mehla, K., & Ramana, J. (2016). Identification of epitope-based peptide vaccine candidates against enterotoxigenic *Escherichia coli*: A comparative genomics and immunoinformatics approach. *Molecular BioSystems, 12*(3), 890–901.

Mustafa, A. S. (2002). Development of new vaccines and diagnostic reagents against tuberculosis. *Molecular Immunology, 39*(1–2), 113–119.

Nagpal, P., Jamal, S., Singh, H., Ali, W., Tanweer, S., Sharma, R., Grover, A., & Grover, S. (2020). Long-range replica exchange molecular dynamics guided drug repurposing against tyrosine kinase PtkA of *Mycobacterium tuberculosis*. *Scientific Reports, 10*(1), 1–11.

Nayak, S. S., Sethi, G., & Ramadas, K. (2023). Design of multi-epitope based vaccine against *Mycobacterium tuberculosis*: A subtractive proteomics and reverse vaccinology based immunoinformatics approach. *Journal of Biomolecular Structure and Dynamics, 41*(23), 14116–14134.

Pablos-Mendez, A., Gowda, D. K., & Frieden, T. R. (2002). Controlling multidrug-resistant tuberculosis and access to expensive drugs: A rational framework. *Bulletin of the World Health Organization, 80*, 489–495 (discussion 495–500).

Park, B. S., Song, D. H., Kim, H. M., Choi, B.-S., Lee, H., & Lee, J.-O. (2009). The structural basis of lipopolysaccharide recognition by the TLR4–MD-2 complex. *Nature, 458*(7242), 1191–1195.

Rapin, N., Lund, O., Bernaschi, M., & Castiglione, F. (2010). Computational immunology meets bioinformatics: The use of prediction tools for molecular binding in the simulation of the immune system. *PLoS ONE, 5*(4), e9862.

Saha, S., & Raghava, G. P. S. (2006). Prediction of continuous B-cell epitopes in an antigen using recurrent neural network. *Proteins: Structure, Function, and Bioinformatics, 65*(1), 40–48.

Sanches, R. C. O., Tiwari, S., Ferreira, L. C. G., Oliveira, F. M., Lopes, M. D., Passos, M. J. F., Maia, E. H. B., et al. (2021). Immunoinformatics design of multi-epitope peptide-based vaccine against *Schistosoma mansoni* using transmembrane proteins as a target. *Frontiers in Immunology, 12*, 490.

Schorey, J. S., & Harding, C. V. (2016). Extracellular vesicles and infectious diseases: New complexity to an old story. *The Journal of Clinical Investigation, 126*(4), 1181–1189.

Sharma, R., Rajput, V. S., Jamal, S., Grover, A., & Grover, S. (2021). An immunoinformatics approach to design a multi-epitope vaccine against *Mycobacterium tuberculosis* exploiting secreted exosome proteins. *Scientific Reports, 11*(1), 1–12.

Trott, O., & Olson, A. J. (2010). AutoDock Vina: Improving the speed and accuracy of docking with a new scoring function, efficient optimization, and multithreading. *Journal of Computational Chemistry, 31*(2), 455–461.

Trunz, B. B., Fine, P. E. M., & Dye, C. (2006). Effect of BCG vaccination on childhood tuberculous meningitis and miliary

tuberculosis worldwide: A meta-analysis and assessment of cost-effectiveness. *The Lancet, 367*(9517), 1173–1180.

Weinreich Olsen, A., Hansen, P. R., Holm, A., & Andersen, P. (2000). Efficient protection against *Mycobacterium tuberculosis* by vaccination with a single subdominant epitope from the ESAT-6 antigen. *European Journal of Immunology, 30*(6), 1724–1732.

Wheeler, D. L., Barrett, T., Benson, D. A., Bryant, S. H., Canese, K., Chetvernin, V., Church, D. M., et al. (2007). Database resources of the National Center for Biotechnology Information. *Nucleic Acids Research, 36*(Suppl. 1), D13–D21.

World Health Organization. (2018). BCG vaccine: WHO position paper, February 2018–recommendations. *Vaccine, 36*(24), 3408–3410.

Yun, J.-S., Kim, A. R., Kim, S. M., Shin, E., Ha, S.-J., Kim, D., & Jeong, H.-S. (2024). In silico analysis for the development of multi-epitope vaccines against *Mycobacterium tuberculosis*. *Frontiers in Immunology, 15*, 1474346.

SUPPLEMENTARY TABLE

Vaccine Sequence:

MKNARTTLIAAAIAGTLVTRSPAGIANADDAGLDPNAAAGPDAVGFDPNLPPAPDAAPVDTPPAPEDA
GFDPNLPPPLAPDFLSPPAEEAPPVPVAYSVNWDAIAQCESGGNWSINTGNGYYGGLQFTAGTWRA
NGGSGSAANASREEQIRVAENVLRSQGIRAWPVCGRRGEAAAKAGLWGNGGSGGAGGNAKKAGLI
GNGGAGGAGGPNKKGSPITTLYVKIDGGTPKKGGMGGSGGGIGAGTTTKKNVPIDPSPDYDASDEIK
KGGTGGAAGLLGWGANGKKRGAVTGPPSPVAAQENKKTVQRQAGCTNDVTINPKKVVANVYTVQR
QAGCTNKKGGVGTTGGAGGNGGGAKKGNSGTANTGFGNAGNVKKTATGIWYLQDRVIVAEKKISTY
FSALLADPTTTPKKNAGAGNTGFFDAGNYNGPGPGYAVAEAATAQSVQQDGPGPGGQEYQAVSAQ
ASAFHGPGPGGNSYAVAEAATAQSVGPGPGRKDIRTTRVTVAPQYGPGPGGGNSYAVAEAATAQS
AAYSTQAKTRAMAAYFMLIGAAFYAAYSGYSGGLYYAAYQAALAMEVYAAYNFMLIGAAFAAYRTYE
ATMSLAAYAAAASTTALAAYYVNTSTTSM

Adjuvant (RPFE) =1-172

14 B-cell epitopes =178-250

5 MHC II (HTL epitopes) = 433-527

5 MHC I (CTL epitopes) = 530-587

3 MHC I (HLA-C epitopes) = 590-623

Linkers

Table 1. Comprehensive Epitope Mapping of Mycobacterium tuberculosis Antigens for Multi-Epitope Vaccine Design

Gene Name	B-Cell Epitope	CTL Epitope	HLA-C Epitope	HTL Epitope
PPE 68		STQAKTRAM (B7,B8,B62) QAALAMEVY (A1,A26,B58,B62)		
Rv0310c	TATGIWYLQDRVIVAE	FMLIGAAFY (A1,A3,A26,B62) NFMLIGAAF (A24,B8,B62)	RTYEATMSL (HLA-C*01:02 HLA-C*03:02 HLA-C*03:03 HLA-C*03:04 HLA-C*04:01 HLA-C*05:01 HLA-C*07:01 HLA-C*07:02 HLA-C*07:04 HLA-C*08:01 HLA-C*08:02 HLA-C*12:02 HLA-C*12:03 HLA-C*15:02 HLA-C*16:01 HLA-C*17:01)	
PE_PGRS35	AGLIGNGGAGGAGGPN GSPITTLYVKIDGGTP GGTGGAAGLLGWGANG ISTYFSALLADPTTTP	SGYSGGLYY (A3,A26,B58,B62)		GQEYQAVSAQASAFH (DRB1_0101 DRB1_0401 DRB1_0405 DRB1_0701 DRB1_0802 DRB1_0901 DRB1_1101 DRB3_0202

Gene Name	B-Cell Epitope	CTL Epitope	HLA-C Epitope	HTL Epitope
				HLA-DQA10501-DQB10301 HLA-DQA10301-DQB10302 HLA-DQA10401-DQB10402 HLA-DQA10102-DQB10602 HLA-DPA10201-DPB11401)
PE_PGRS31	AGLWGNGGSGGAGGNA GGMGGSGGGIGAGTTT		AAAASTTAL (HLA-C*01:02 HLA-C*03:02 HLA-C*03:03 HLA-C*03:04 HLA-C*05:01 HLA-C*07:04 HLA-C*08:01 HLA-C*08:02 HLA-C*12:02 HLA-C*15:02 HLA-C*16:01 HLA-C*17:01)	YAVAEAATAQSVQQD (HLA-DQA10501-DQB10201 HLA-DQA10501-DQB10301 HLA-DQA10301-DQB10302 HLA-DQA10401-DQB10402 HLA-DQA10102-DQB10602)
	GGVGTTGGAGGNGGGA			GNSYAVAEAATAQSV (DRB1_0101 DRB1_1101 DRB3_0202 HLA-DQA10501-DQB10301 HLA-DPA10201-DPB11401)
				GGNSYAVAEAATAQS (DRB1_0405 DRB1_0701 DRB1_0802 DRB1_0901 HLA-DQA10501-DQB10201 HLA-DQA10301-DQB10302 HLA-DQA10401-DQB10402)
lpqG				RKDIRTTRVTVAPQY (DRB1_0401 DRB1_0701 DRB1_0802 DRB4_0101 HLA-DQA10301-DQB10302 HLA-DQA10401-DQB10402 HLA-DQA10102-DQB10602 HLA-DPA10201-DPB11401)
PPE39	GNSGTANTGFGNAGNV NAGAGNTGFFDAGNYN		YVNTSTTSM (HLA-C*02:02 HLA-C*02:09 HLA-C*03:02 HLA-C*03:03 HLA-C*03:04 HLA-C*08:02 HLA-C*12:02 HLA-C*12:03	

Gene Name	B-Cell Epitope	CTL Epitope	HLA-C Epitope	HTL Epitope
			HLA-C*15:02 HLA-C*16:01 HLA-C*17:01)	
Rv1975	NVPIDPSPDYDASDEI			
	RGAVTGPPSPVAAQEN			
	TVQRQAGCTNDVTINP			
	VVANVYTVQRQAGCTN			

Table 2. Docking results (PyDock) Vaccine construct with TLR4

RMSD from the overall lowest-energy structure	0.248
Van der Waals energy	42.436
Electrostatic energy	-10.009
Desolvation energy	-49.937
Z-Score	-1.10

Table 3. Vaccine construct with MHC I

RMSD from the overall lowest-energy structure	0.248
Van der Waals energy	81.423
Electrostatic energy	-19.16
Desolvation energy	-32.681
Z-Score	-2.89

Peer-review history:
The peer review history for this paper can be accessed here:
https://pr.sdiarticle5.com/review-history/147582